Mach-Zehnder Modulator using Membrane InGaAsP Phase Shifters and SOAs inside Interferometer Arms on Si Photonics Platform

Takuma Aihara, Tatsurou Hiraki, Takuro Fujii, Koji Takeda, Takaaki Kakitsuka, Tai Tsuchizawa, and Shinji Matsuo
NTT Device Technology Labs, NTT Corporation, 3-1 Morinosato-Wakamiya, Atsugi, Kanagawa 243-0198, Japan
Author e-mail address: takuma.aihara.vp@hco.ntt.co.jp

Abstract: A Mach-Zehnder modulator having III-V membrane phase shifters and semiconductor optical amplifiers inside interferometer arms is heterogeneously integrated with Si waveguides. The device exhibits 6-dBm fiber output power and 40-Gbit/s NRZ modulations with clear eye-openings.

1. Introduction

With the rapid increase in internet traffic, there is a growing demand for high-capacity optical transmitters. Large-scale photonic integrated circuits (PICs) on a Si substrate are essential for building such high-capacity optical transmitters with size and cost saving. A Mach-Zehnder modulator (MZM) is an important element because it provides high throughput by using both amplitude and phase modulations. In this context, large-scale PICs using MZMs have attracted much attention. Si-based MZMs have been integrated with polarization rotators, polarization beam splitters, optical filters, and spot-size converters (SSCs) on a Si substrate [1]. However, the poor modulation efficiency of Si phase shifters results in large optical and electrical losses in MZMs. In addition, waveguide loss and chip-to-fiber coupling loss are still remaining problems. All these issues limit the further development of optical transmitters on a Si substrate in terms of footprint, fiber output power, and power consumption.

The use of III-V materials on Si is a promising solution because they provide efficient optical phase modulation and amplification. Recently, heterogeneously integrated III-V devices such as phase shifters and semiconductor optical amplifiers (SOAs) on Si have been developed by employing direct bonding techniques [2,3]. However, integration with both SOAs and phase shifters has still an issue because they require different bandgap materials.

For SOA integration with MZMs, the position of the SOA is important. An SOA in a pre-amplifier configuration, where the light is input into the SOA before passing through the MZM, has an advantage in terms of signal quality because light input into the SOA is continuous-wave (CW) light. On the other hand, output power is relatively small because there are the phase shifter loss, waveguide loss, and chip-to-fiber coupling loss after passing through the SOA. On the other hand, an SOA in a post-amplifier configuration, where the light is input into the SOA after passing through the MZM, can provide higher output power compared with the pre-amplifier one. However, since the intensity-modulated signal inputs into the SOA, the signal quality is degraded when the SOA is operated in the saturation region.

We have fabricated a high-efficiency MZM using InGaAsP bulk-core membrane phase shifters and a low-power-consumption SOA on Si substrate [4]. Since the fabricated device constructs the pre- or post- amplifier configuration, there is remaining tradeoff relationship described above. In this paper, we propose new configuration of an MZM using SOAs, in which an SOA is placed behind a phase shifter and inside the interferometer arm. In this configuration, the input optical power into SOA becomes low compared with the pre-amplifier configuration due to the splitting of the input CW light and the losses of the phase shifter and waveguide, and its change is relatively low. To integrate different bandgap III-V materials, we employed the regrowth of III-V materials on Si substrate, which is the same fabrication procedure for PICs on InP substrate. The key to realizing regrowth with high-quality epitaxial layers on Si substrate is its thickness, and the total thickness of III-V layers must be less than the critical thickness, typically ~430 nm. In a fabricated device with this configuration, we achieved high fiber output power of 6-dBm, which is ~6 dB incensement from previous result where the SOA is used as a pre-amplifier. We also demonstrated 40-Gbit/s non-return-to-zero (NRZ) modulations with clear eye opening.

2. Design and fabrication

Figure 1(a) shows a schematic of a device configuration on a Si substrate. The MZM consists of Si multi-mode interferometers (MMIs), membrane InGaAsP bulk phase shifters, and membrane InGaAsP-based multiple-quantum well (MQW) SOAs, in which Si waveguides connect each element. The device has SiO_x waveguides for fiber-to-chip coupling. A 500-µm-long phase shifter and 300-µm-long SOA with photoluminescence (PL) peak wavelengths of 1.3 and 1.5 µm, respectively, are integrated inside the interferometer arm. Note that the optical input power into the SOA is relatively low because the input light passes through the fiber-to-chip coupler (SiO_x waveguide), 3-dB divider (MMI), and phase shifter. In addition, inside the interferometer arm, almost ideal phase change with little intensity change is generated. As a result, high-output power can be expected with suppression of signal degradation by pattern effect. Figure 1(b) and (c) are cross-sectional views of the phase shifter and SOA. The phase shifter consists of an InGaAsP core region buried in a 230-nm-thick InP layer, and it has a lateral *p-n* junction. When a reverse bias voltage is applied to the lateral *p-n* junction, the refractive index is changed by the carrier plasma effect, band filling effect, and Frantz-Keldysh effect. The membrane structure enables high optical confinement in the InGaAsP core, which results in the improvement of modulation efficiency. Note that there is no Si waveguide to increase the optical confinement in InGaAsP core. The SOA consists of an InGaAsP-based MQW core region buried in a 230-nm-thick InP layer, and it has a lateral *p-i-n* junction. The optical confinement can be controlled by the width of the Si waveguide for designing the characteristics of SOA in terms of the power consumption and the maximum output power. We set the Si waveguide width to 640 nm and filling factor in six period quantum wells to 6%. The membrane structure with a small active area provides the small injection current for the required optical gain, resulting in low power consumption even when we employ two SOAs. Figure 1(d) shows the calculated light transition from the Si waveguide to the SOA via the 50-µm length and 100-nm tip width InP taper waveguide. As shown in this, the light transition with low loss was confirmed. This is another advantage of the membrane structure, which is low-loss optical coupling to a 220-nm-thick Si waveguide using a short-length tapered InP waveguide because of the index matching between them.

The fabrication procedure of the device with different bandgap materials on Si substrate is as follows. An InP substrate containing the MQWs is bonded to a Si substrate containing the Si waveguide circuits. After InP substrate removal, the MQW layer is etched except for the SOA regions, and then an InGaAsP bulk layer is grown for the phase shifter. The MQW layer and bulk layer are etched to form their cores, and the InP is regrown to form buried heterostructures (BHs). The details of the fabrication process are described in Ref [4].

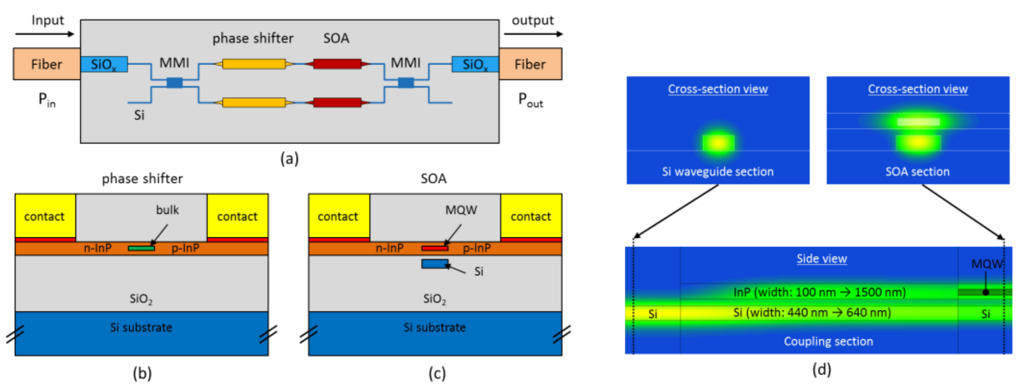

Fig. 1. Schematics of (a) top-view of device configuration, cross-sectional view of (b) phase shifter and (c) SOA. (d) Calculated light transition from Si waveguide to SOA via InP taper waveguide.

3. Results and discussions

For device characterization, high-numerical-aperture fibers (HNAFs) were physically connected to the SiO_x waveguides. Figure 2(a) shows the measured optical spectrum from the integrated device, where a laser beam with -10-dBm power and a wavelength of 1.55 µm was input to the device with transverse electric field polarization and the bias current of the SOAs was set to 62 and 57 mA to maximize fiber output power. As shown in this figure, we observed an amplified spontaneous emission (ASE) peak at a center wavelength of 1.52 µm. Note that there is no lasing peak around the ASE peak. This indicates that reflections within the chip and at the chip edges are sufficiently small. The small reflections are thanks to the narrow-tip-width tapered InP waveguide on the 220-nm-thick Si waveguide as shown in Fig. 1(d), and index matching between the SiO_x waveguide and HNAF. Next, fiber input power versus output power was measured. As shown in Fig. 2(b), the output power is linearly proportional to the input power up to ~5 dBm, which is high compared with an SOA used as a pre-amplifier. Thanks to the optical gain provided by the SOAs, fiber-to-fiber transmittance (P_{out}/P_{in}) of -2.3 dB was obtained despite the optical loss, including that of the two fiber-to-chip couplings (6.8 dB) and the MZM. Beyond the input power of ~5 dBm, the output power turns off due to gain saturation. However, in the saturation region, a high-fiber output power of 6 dBm was obtained for a fiber input power of 11 dBm.

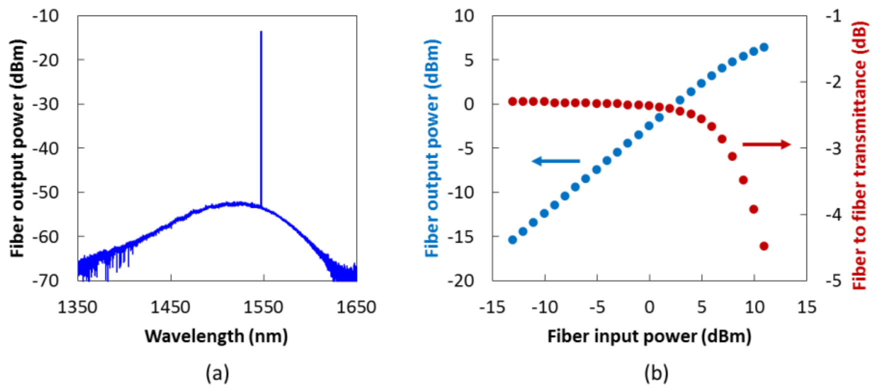

Fig. 2. (a) Measured optical spectrum with -10-dBm input and (b) fiber output power versus fiber input power.

Finally, we measured the dynamic characteristics of the device. Figure 3(a) shows the experimental setup. The electrical signals were input from the pulse pattern generator (PPG) through the linear amplifier. The output light from the device was amplified by the erbium doped fiber amplifier (EDFA). The *p-i-n* photodetector was used for the signal detection. Figure 3 shows the eye diagram with 28- and 40-Gbit/s NRZ signals with a 2^{31}-1 PRBS for fiber input power of 11 dBm, where SOA was operated in saturation region. The dynamic extinction ratios were 4.3 and 3.8 dB for 28 and 40 Gbit/s, respectively. As shown in Fig. 3(b) and (c), a significant pattern effect was not observed despite that SOAs were operated in the saturation region. These results indicate that the advantages of our proposed configuration which can suppress intensity change. SOAs were operated in the saturation region. These results indicate that the advantages of our proposed configuration which can suppress intensity change.

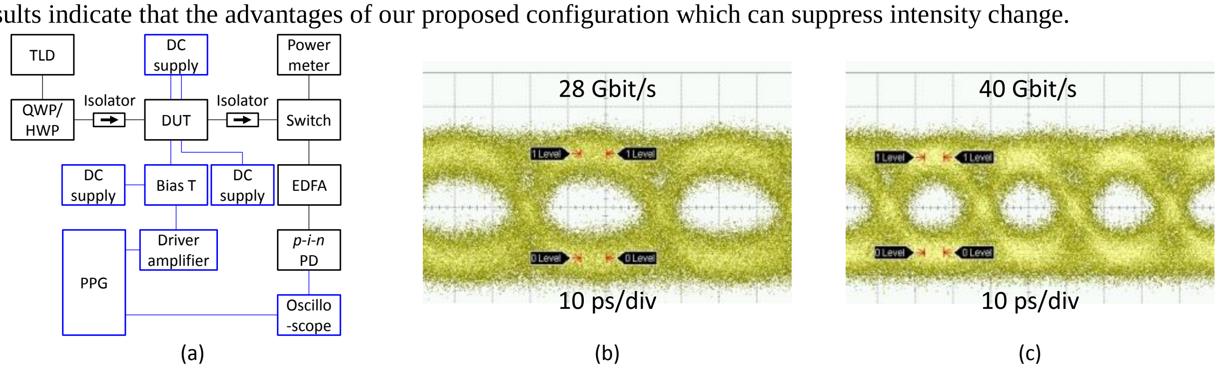

Fig. 3. (a) Experimental setup and measured eye diagrams for NRZ with (b) 28 and (c) 40-Gbit/s signals.

4. Conclusion

We have demonstrated an MZM on Si substrate consisting of different-bandgap membrane InGaAsP core phase shifters and SOAs inside the interferometer arms. The device was fabricated by using a regrowth process on Si substrate. The device exhibits 6-dBm fiber output power and 40-Gbit/s NRZ modulations with clear eye opening.

5. References

[1] C. R. Doerr, "Silicon photonic integration in telecommunications," Frontiers in Physics, **3**, 37, 1–16, 2015.

[2] M. L. Davenport, S. Skendzic, N. Volet, J. C. Hulme, M. J. R. Heck, J. E. Bowers, "Heterogeneous Silicon//III-V Semiconductor Optical Amplifiers," IEEE J. Select. Top. QE, **22**, 6, 3100111, 2016.

[3] T. Hiraki, T. Aihara, K. Takeda, T. Fujii, T. Kakitsuka, T. Tsuchizawa, H. Fukuda, and S. Matsuo, "Membrane InGaAsP Mach-Zehnder modulator with SiN:D waveguides on Si platform," Opt. Express **27**, 13, 18612–18619, 2019.

[4] T. Hiraki, T. Aihara, T. Fujii, K. Takeda, T. Kakitsuka, T. Tsuchizawa, and S. Matsuo, "Loss-less operation of membrane III-V semiconductor Mach-Zehnder modulator with optical amplifier on Si platform," ECOC2019, Proc. Int. Conf. ECOC, Dublin, Ireland, September 2019, Tu.2.A.2.